Mechanics of large folds in thin interfacial films

Vincent Démery,* Benny Davidovitch, and Christian D. Santangelo
Department of Physics, University of Massachusetts, Amherst, Massachusetts 01003, USA
(Received 14 August 2014; published 14 October 2014)

A thin film confined to a liquid interface responds to uniaxial compression by wrinkling, and then by folding, that has been solved exactly before self-contact. Here, we address the mechanics of large folds, i.e., folds that absorb a length much larger than the wrinkle wavelength. With scaling arguments and numerical simulations, we show that the antisymmetric fold is energetically favorable and can absorb any excess length at zero pressure. Then, motivated by puzzles arising in the comparison of this simple model to experiments on lipid monolayers or capillary rafts, we discuss how to incorporate film weight, self-adhesion, or energy dissipation.

DOI: 10.1103/PhysRevE.90.042401 PACS number(s): 68.60.Bs, 46.32.+x, 46.70.−p, 89.75.Kd

I. INTRODUCTION

Deforming soft two-dimensional objects by means of capillarity opened a new route to design three-dimensional structures at the micro- and nanoscale [1–3]. However, attaching these thin films to soft substrates submits them to a wealth of morphological instabilities such as wrinkling, crumpling, or folding [4]. Such instabilities have been observed in lipid monolayers [5–12], nanoparticles films [13], capillary rafts [14–16], and thin polymer sheets resting on a gel [17,18] or a liquid substrate [19,20]. Their complete characterization is a necessary step toward their control and use in the fabrication of small structures.

A simple setup where some of these instabilities arise consists of a thin film at an initially flat liquid interface that is confined in one horizontal direction (see Fig. 1). The film responds to confinement by wrinkling and folding in a universal way resulting from the competition between the bending energy to deform the film and the gravitational energy to lift the liquid [17], the wrinkle-to-fold transition being associated with a buckling localization [21]. Minimizing the total energy leads to an integrable equation for the shape of the film [22–24], allowing one to obtain an analytical expression for the energy as a function of the confinement length. However, this exact result holds only up to self-contact of the film, and that occurs as soon as the confinement length reaches approximately the wavelength of the wrinkles [22].

On the other hand, the experimental range of confinement for lipid monolayers [5,6,9–12] and capillary rafts [15,16] goes far beyond self-contact. In the first case, folds are formed [5] abruptly, causing jerky monolayer dynamics [10]. In a folding event, a length $\sim 2\,\mu$m is absorbed in a fold in ~ 0.1 s. It has already been noted that this characteristic time is anomalously fast [25], but what sets the characteristic length is also unclear. In capillary rafts, large folds—involving a length much larger than the wrinkle wavelength—are formed and eventually get destabilized under their own weight [15]. To understand the behavior of the film in these experiments, a systematic study of the mechanics of large folds is required. In this article, we address the following questions: what is the shape of a fold after self-contact? What is its energy?

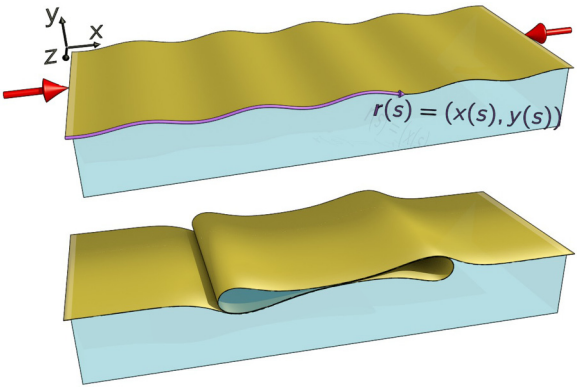

FIG. 1. (Color online) A thin interfacial film responds to uniaxial confinement first by wrinkling (top) and then by forming a large fold (bottom). The invariance of the system along $\hat{\boldsymbol{z}}$ allows us to parametrize the shape of the film by a function $\boldsymbol{r}(s) = [x(s), y(s)]$.

II. MODEL

A thin film at a liquid interface is submitted to uniaxial confinement along $\hat{\boldsymbol{x}}$; the system is invariant in the $\hat{\boldsymbol{z}}$ direction (see Fig. 1). Soon after the confinement length exceeds a threshold value for wrinkling instability, the film responds as if it was nearly inextensible, and can be modeled as a rod parametrized by $\boldsymbol{r}(s) = (x(s), y(s))$ in a vertical plane (s is the arc length). Pocivavsek *et al.* [17] found that the bending energy of the film and the gravitational energy of the displaced fluid are responsible for the wrinkle-to-fold transition. Those energies are, respectively,

$$U_{\text{bend}} = \frac{B}{2}\int \boldsymbol{r}''(s)^2 ds, \tag{1}$$

$$U_{\text{grav}} = \frac{\rho g}{2}\int y(s)^2 x'(s) ds, \tag{2}$$

where B is the bending modulus of the film, ρ is the mass density difference between the fluids below and above the sheet, g is the gravitational acceleration, and energies are given per unit length in the orthogonal direction. For a continuous material, the bending modulus is given by $B = Et^3/[12(1-\nu^2)]$, where E is the Young modulus, ν the Poisson ratio, and t the thickness of the film. These parameters allow one to define the characteristic length $l = (B/\rho g)^{1/4}$. In

*vdemery@physics.umass.edu

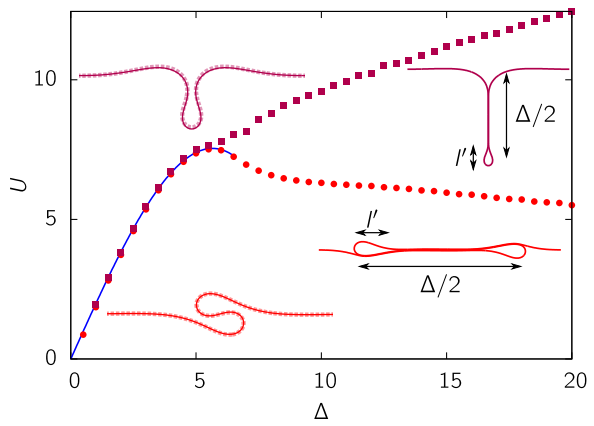

FIG. 2. (Color online) Fold energy as a function of the imposed displacement for the symmetric (squares) and antisymmetric (circle) folds. The solid blue line is the exact solution, Eq. (3), valid before self-contact. Symmetric (top) and antisymmetric (bottom) configurations are shown before self-contact (left, exact solutions from Diamant and Witten [22] are shown as thick dashed lines) and after self-contact (right). After self-contact, the size of the fold $\Delta/2$ absorbs the excess length, while bending is localized in highly curved zones of length l'.

the following, we rescale lengths by l and energies by B/l such that we are left with dimensionless quantities only. We focus on the dependence of the energy on the confinement length $\Delta = L - [x(L) - x(0)]$, which is the only dimensionless parameter in the problem (L is the length of the film in the confined direction). In this study, we assume that the length of the film in the confined direction, L, is large enough so that boundary conditions do not affect the behavior of the system; clamped boundary conditions have been shown to select the folding mode if L is of order 1 [26].

The system defined by the energies Eqs. (1) and (2) is integrable [22–24]. For a given confinement length Δ, there is a continuous family of solutions with the same energy,

$$U^0(\Delta) = 2\Delta - \frac{\Delta^3}{48}, \tag{3}$$

among which are the symmetric and antisymmetric configurations pictured in Fig. 2. Two points are noteworthy: first, this energy is always lower than the energy of the wrinkled state, $U^{\mathrm{wr}} = 2\Delta$ [6]; second, this energy has a maximum and may even become negative. This is prevented by self-contact, where the exact solutions cease to be valid. Self contact occurs at $\Delta \simeq 5.6$ for the symmetric fold, just before the maximum, and at $\Delta \simeq 6.6$ for the antisymmetric fold, just after U^0 reaches its maximum, meaning that there exists an antisymmetric fold with negative pressure.

III. SCALING ARGUMENTS AND NUMERICAL SOLUTION

We start our investigation of large folds with a scaling analysis. Large symmetric and antisymmetric folds are depicted in Fig. 2. A fold is characterized by two lengths: its size $\Delta/2$ that is given by the confinement length (assuming that the whole confinement length is absorbed into the fold), and the size l' of the highly curved zone(s) that contains bending. The size l' is determined by an energy balance. In the symmetric case, the bending and gravitational energies are, respectively, $1/l'$ and $\Delta l'^2$ (the volume of fluid contained in the highly curved zone is l'^2 and its displacement is Δ). Minimizing over l' gives $l' \sim \Delta^{-1/3}$ and the scaling law

$$U^{\mathrm{sym}} \sim \Delta^{1/3}. \tag{4}$$

Note that this scaling is strictly different from the result of a scaling argument in Pocivavsek *et al.* [17], which neglected the effect of self-avoidance. On the other hand, in the antisymmetric case, the displacement of the fluid inside the highly curved zones does not depend on the fold size Δ. The bending and gravitational energies are, respectively, $1/l'$ and l'^3, leading to $l' \sim 1$ and

$$U^{\mathrm{antisym}} \sim 1. \tag{5}$$

Since the fold occurs at $\Delta > 1$, the antisymmetric fold has a lower energy than the symmetric one, which does not depend on the size of the fold: once it is formed, it can absorb length at negligible cost.

In order to completely characterize the behavior of the fold, we have to investigate the crossover between the energy at self-contact, given by Eq. (3), and the asymptotic behaviors of Eqs. (4) and (5). Besides this crossover, we want to determine the asymptotic value of the energy of the asymmetric fold. We resort to a numerical computation of the film shape to answer these questions.

The rod parametrized by $\boldsymbol{r}(s)$ is modeled as a chain of beads with bending and gravitational energies, a stretching energy with a very large stretching modulus and a short-range repulsion energy between the beads to prevent self-crossing; the expression of these energies and more details about the simulations are given in the Appendix. The equilibrium rod configuration is given by minimization of the full energy, and its energy is computed with the bending and gravitational contributions only. Another way to obtain the shape of the film would have been to solve exactly the equations for its shape between points of self-contact; this has been done in a similar configuration [27], but it was limited to one self-contact point and in our case finite portions of the film are in self-contact. We perform two kinds of simulations: in the first, we find the energy minimizing configuration of the complete rod; in the second, we consider one half of the rod and impose a symmetric configuration. In the first case, the energy minimizing configuration is always found to be antisymmetric after self-contact. To check the validity of the numerical scheme, we compare the symmetric and antisymmetric shapes of the rod given by our simulations before self-contact to the exact solutions of Diamant and Witten [22] in Fig. 2; an excellent agreement is found.

The energies of the symmetric and antisymmetric configurations are plotted as a function of the displacement in Fig. 2: they are equal before self-contact and differ strongly after self-contact. The energy of the symmetric fold keeps increasing while that of the antisymmetric fold decreases monotonously to a plateau well below its maximum value (the symmetric fold shown in Fig. 2 is pointing down, but the corresponding configuration with the fold pointing up has the same energy).

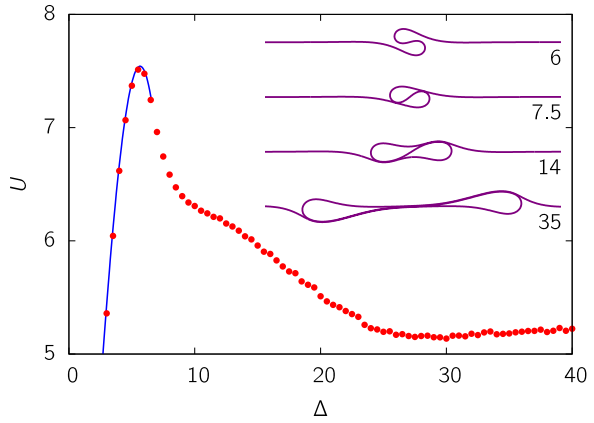

FIG. 3. (Color online) Energy of the antisymmetric fold as a function of the confinement length Δ. Red circles are the results of the numerical simulations, the continuous line is the exact solution, Eq. (3), which is valid before self-contact, i.e., for $\Delta \lesssim 6.6$. Inset: typical configurations showing the different folding steps (numbers indicate the confinement length).

Before self-contact, the fold shape is given by any solution in the continuous family of solutions with the same energy. When self-contact occurs, the self-contact point slides, driving the fold toward the antisymmetric state. Then, the film stays in the antisymmetric configuration and the highly curved zones get larger, and later start to move apart until a trilayer is formed between them. Once the trilayer is formed, it can expand at zero-energy cost, without any change in the shape of the highly curved zones. This steps are represented in the inset of Fig. 3.

The transition from the flat to the folded film resembles the monolayer-to-trilayer transition observed in nanospheres rafts [13].

IV. DISCUSSION

The picture that emerges from our analysis is that large folds are antisymmetric and energetically cheap; it does not fit the observations of folds in capillary rafts or in lipid monolayers:

(i) folds in capillary rafts are often symmetric [15,16];

(ii) folds in lipid monolayers have a well-defined length; i.e., creating several folds is favorable to enlarging one fold [10].

These discrepancies indicate that the energetic consideration of bending and gravity alone do not account for the observed properties: other effects should be involved. As a preliminary exploration of such effects, we discuss possible extensions of the simple model used here and their potential effect on the energy and dynamics of large folds.

The film weight plays a crucial role in capillary rafts, leading to fold instability and breaking [15,16]. Here, we discuss its effect on the shape and energy of the fold. The film weight enters in the energy via an additional term,

$$U_{\text{weight}} = M \int y(s)\, ds, \tag{6}$$

where $M = \rho_f [g/(B\rho^3)]^{1/4}$ and ρ_f is the effective mass of the film per unit area (taking into account its buoyancy). It is noteworthy that for the very small deformations involved in the wrinkled phase, the gravitational energy is approximated by $U_{\text{grav}} \simeq (1/2) \int y(s)^2\, ds$; thus, the film weight can be absorbed in a shift of the y coordinate and has no effect. For large folds, it is straightforward to incorporate it into the scaling analysis: it contributes to the downward symmetric fold (that is selected if $\sigma > 0$) as $U_{\text{weight}} \sim -M\Delta^2$ and it does not contribute to the antisymmetric fold. This negative contribution may thus make the symmetric fold favorable and even unstable since its energy $U^{\text{sym}} \sim \Delta^{1/3} - M\Delta^2$ decreases to $-\infty$ after its maximum at $\Delta_c \sim M^{-3/5}$. Moreover, a tension $T \sim \Delta$ is induced in the film that will eventually break; this behavior is observed in heavy capillary rafts [15,16]. On the other hand, for monolayers, a rough estimate gives $M \simeq 10^{-3}$ in dimensionless units, meaning that the weight of the film may have an effect only when $\Delta_c \simeq 100$, i.e., for very large folds. A strong effect of the weight of the monolayers on their folding is thus unlikely.

We turn to self-attraction, which can hold two parts of the fold together [19] and has been suggested as a mechanism to drive the folding of lipid monolayers [12]. It can be modeled by an energy gain Γ per unit area of the film in contact with itself. The adhesion energy Γ may differ on either side of the film: not only the two sides of the film can be different, as is the case for lipid monolayers, but the interaction of the film with itself can depend on the surrounding liquid. The symmetric fold is the first to experience self-contact; thus, it may be favored in the presence of self-attraction. Self attraction leads to an energy gain $\Gamma\Delta$, giving $U^{\text{sym}} \sim \Delta^{1/3} - \Gamma\Delta$. Thus, depending on Γ, the film may be unstable at self-contact. In case self-adhesion prevents relative motion and fluid flow between two sections of the film in contact with each other, the size of the highly curved zone cannot decrease as $l' \sim \Delta^{-1/3}$ (it requires fluid flow from the highly curved zone to the upper reservoir) and remains equal to its value at self-contact, $l' \sim 1$, resulting in the total energy $U^{\text{sym}} \sim (1 - \Gamma)\Delta$. Let us now consider the antisymmetric fold, with self-attraction on the two sides: the energy gain is higher than in the symmetric case (although self-contact occurs later), but relative motion of sticking parts is required; thus, if the upper fluid is sufficiently viscous, the symmetric fold is preferable. If only one side experiences self-attraction, the relative motion of sticking parts can be avoided, the energy gain is the same as in the symmetric case but the gravitational cost (of the liquid phase) is lower: the antisymmetric fold is still favored.

Last, energy dissipation may occur during the fold formation due to flow between nearly touching parts of the film (symmetric fold) or the relative motion of nearly touching parts of the film (antisymmetric fold). When the symmetric fold grows, the highly curved zone shrinks as $l' \sim \Delta^{-1/3}$ under the effect of increasing hydrostatic pressure and an upward flow is generated in the narrow neck formed by the two parts of the film that are close to self-contact. The radius of the highly curved zone shrinks slowly; thus, the dissipation decreases as the fold size increases. In the antisymmetric fold, the effect is slightly different: the length of the highly curved zones does not change, but proximal parts of the film are in relative motion (in Fig. 3, inset $\Delta = 35$, the top part of the trilayer moves left, the center part does not move, and the bottom part moves right). A flow is needed to lubricate this relative motion, and the dissipation increases as Δ, the length of the

portions of the film in self-contact. Hence, energy dissipation will be lower in the symmetric fold, and hence it is favored if the formation of the fold is rapid. Once formed, the symmetric fold will eventually relax to the antisymmetric configuration. A more precise analysis of the sources of energy dissipation would consider the effect of self-attraction, that may reduce the thickness of the fluid layer between parts of the film and thus increase dissipation.

V. CONCLUSION

We have investigated the behavior of large folds that may appear in thin interfacial films under uniaxial confinement. Under the assumption that the system is controlled by bending and gravity [17], we have shown that the large folds are antisymmetric and their energy decreases after a maximum reached before self-contact to a universal value well below this maximum (see Fig. 3). The antisymmetric folds are energetically cheap—one fold can absorb all the excess length at a finite cost—and stable—they do not unfold spontaneously at zero tension. On the other hand, the energy of symmetric folds increases monotonously, and these folds are thus less favorable energetically.

Although antisymmetric folds may be the actual cause of "trilayers," which have been observed, for instance, by Leahy *et al.* [13], their actual development for the wrinkled state had not been directly observed. We have shown that they do not explain the preferred fold size observed in compressed lipid monolayers [10]. Together with the kinetic puzzle encountered in trying to predict the folding timescale of monolayers [25], this suggests that other interactions must be included in the model. We discussed the effect of the weight of the film, its self-attraction, and energy dissipation, finding that the symmetric fold may be favored in some cases. A more thorough study of these effects is, however, needed to draw quantitative predictions on the modifications of the folding behavior presented here.

On the other hand, Rivetti and Antkowiak [23,28] have observed the exact solutions of the model presented here [22–24]. The large size system—the characteristic length is $l \sim 1\,\mathrm{cm}$—used in their experiment appears to be accurately described by bending and gravity only, and is thus likely to exhibit the folding behavior predicted here.

ACKNOWLEDGMENTS

V.D. thanks S. Protière and M. Abkarian for stimulating discussions about the shape and stability of folds appearing in confined granular rafts, A. Evans, A. R. C. Romaguera, and J. Paulsen for useful advices on the numerical computations, and M. Rivetti for insightful comments. The authors acknowledge financial support by the KECK foundation Award 37086 (V.D. and C.S.) and NSF CAREER Award DMR-11-51780 (B.D.).

APPENDIX: DETAILS OF THE NUMERICAL SIMULATIONS

The rod is modeled by a chain of N beads located at $\boldsymbol{r}_i = (x_i, y_i)$ (see Fig. 4) interacting via bending, gravitational, stretching, and self-avoidance energies, defined, respectively, by

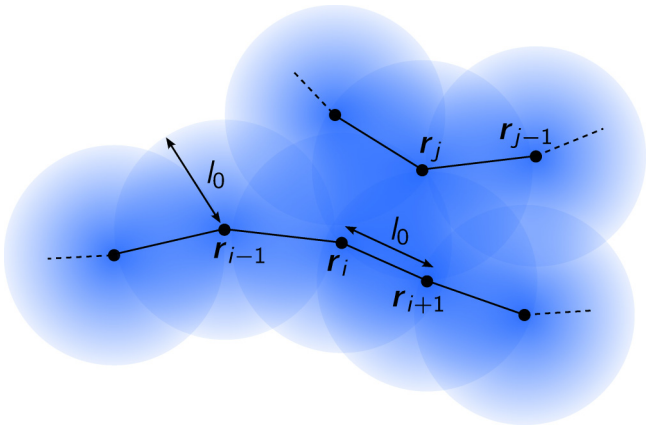

FIG. 4. (Color online) Discretized model used for the simulations. The shaded discs represent the repulsion interaction, the range of which is given by the rest length l_0 between two neighbors to prevent self-crossing between two parts of the rod.

$$U_{\mathrm{bend}} = \frac{1}{2l_0^3}\sum_i (\boldsymbol{r}_{i+1} - 2\boldsymbol{r}_i + \boldsymbol{r}_{i-1})^2, \tag{A1}$$

$$U_{\mathrm{grav}} = \frac{1}{2}\sum_i \frac{y_i + y_{i+1}}{2}(x_{i+1} - x_i), \tag{A2}$$

$$U_{\mathrm{stretch}} = \frac{S}{2l_0^3}\sum_i \left[(\boldsymbol{r}_{i+1} - \boldsymbol{r}_i)^2 - l_0^2\right], \tag{A3}$$

$$U_{\mathrm{avoid}} = A\sum_{j\geqslant i+2} \max(l_0 - |\boldsymbol{r}_i - \boldsymbol{r}_j|, 0). \tag{A4}$$

The bending and gravitational energies are a direct discretization of Eqs. (1) and (2). The rest distance l_0 between two neighboring beads also defines the range of the repulsion between the beads (in order not to modify the elastic properties of the rod, only beads with an index difference larger than the range are interacting). The stretching modulus is set to $S = 1\,000$ to model unstretchability and the self-avoidance parameter is set to $A = 1$, which is enough to prevent self-crossing; changing these parameters (e.g., increasing S or A) does not affect the simulations results. $N = 3\,265$ beads are used to model a rod of length $L = Nl_0 = 120$, such that the fixed ends are far away from the fold.

The total energy is minimized using the conjugate gradient descent implemented in the GNU Scientific Library [29]. The self-avoidance generates effective friction between parts of the rod that are pushed against each other by the fluid, hindering direct convergence to the ground state in the minimization. To solve this problem, after minimizing the energy with $N = N_0 = 3265$ beads, the rod is discretized with a different random number of beads $N \simeq N_0$ (keeping the overall shape) and the energy is minimized again. Repeating these steps, that amount to "shake" the beads along the rod, introduces fluctuations that allow to overcome friction and finally reach the ground state. Once the ground state of the total energy is found, its energy is computed with the bending and gravitational energies only.

To find the symmetric fold shape, one half of the rod ($x > 0$) is simulated. Repulsion from the symmetry plane $x = 0$ ($U_{\text{repulsion}} = A \sum_j \max(l_0 - x_j, 0)$) is enough to prevent self-crossing.

The simulations results converge when the number of beads is increased and are successfully compared to the exact solutions of Diamant and Witten [22] before self-contact is reached (see Fig. 2).

[1] C. Py, P. Reverdy, L. Doppler, J. Bico, B. Roman, and C. N. Baroud, Phys. Rev. Lett. **98**, 156103 (2007).
[2] B. Roman and J. Bico, J. Phys. Condensed Matter **22**, 493101 (2010).
[3] T. G. Leong, A. M. Zarafshar, and D. H. Gracias, Small **6**, 792 (2010).
[4] B. Li, Y.-P. Cao, X.-Q. Feng, and H. Gao, Soft Matter **8**, 5728 (2012).
[5] H. E. Ries, Nature **281**, 287 (1979).
[6] S. T. Milner, J. F. Joanny, and P. Pincus, Europhys. Lett. **9**, 495 (1989).
[7] A. Saint-Jalmes and F. Gallet, Eur. Phys. J. B: Condensed Matter Complex Syst. **2**, 489 (1998).
[8] C. Ybert, W. Lu, G. Möller, and C. M. Knobler, J. Phys. Chem. B **106**, 2004 (2002).
[9] Y. Zhang and T. M. Fischer, J. Phys. Chem. B **109**, 3442 (2005).
[10] A. Gopal, V. A. Belyi, H. Diamant, T. A. Witten, and K. Y. C. Lee, J. Phys. Chem. B **110**, 10220 (2006).
[11] G. Pu, M. A. Borden, and M. L. Longo, Langmuir **22**, 2993 (2006).
[12] K. Y. C. Lee, Ann. Rev. Phys. Chem. **59**, 771 (2008).
[13] B. D. Leahy, L. Pocivavsek, M. Meron, K. L. Lam, D. Salas, P. J. Viccaro, Ka Yee C. Lee, and B. Lin, Phys. Rev. Lett. **105**, 058301 (2010).
[14] D. Vella, P. Aussillous, and L. Mahadevan, Europhys. Lett. **68**, 212 (2004).
[15] S. Protière, M. Abkarian, J. Aristoff, and H. Stone (2010), arXiv:1010.3205.
[16] M. Abkarian, S. Protière, J. M. Aristoff, and H. A. Stone, Nat. Commun. **4**, 1895 (2013).
[17] L. Pocivavsek, R. Dellsy, A. Kern, S. Johnson, B. Lin, K. Y. C. Lee, and E. Cerda, Science **320**, 912 (2008).
[18] F. Brau, P. Damman, H. Diamant, and T. A. Witten, Soft Matter **9**, 8177 (2013).
[19] D. P. Holmes and A. J. Crosby, Phys. Rev. Lett. **105**, 038303 (2010).
[20] H. King, R. D. Schroll, B. Davidovitch, and N. Menon, Proc. Natl. Acad. Sci. USA **109**, 9716 (2012).
[21] B. Audoly, Phys. Rev. E **84**, 011605 (2011).
[22] H. Diamant and T. A. Witten, Phys. Rev. Lett. **107**, 164302 (2011).
[23] M. Rivetti, Comptes Rendus Mécanique **341**, 333 (2013).
[24] H. Diamant and T. A. Witten, Phys. Rev. E **88**, 012401 (2013).
[25] N. Oppenheimer, H. Diamant, and T. A. Witten, Phys. Rev. E **88**, 022405 (2013).
[26] M. Rivetti and S. Neukirch, J. Mech. Phys. Solids **69**, 143 (2014).
[27] G. Domokos, W. B. Fraser, and I. Szeberényi, Physica D: Nonlinear Phenomena **185**, 67 (2003).
[28] M. Rivetti and A. Antkowiak, Soft Matter **9**, 6226 (2013).
[29] B. Gough, *GNU Scientific Library Reference Manual*, 3rd ed. (Network Theory Ltd., Bristol, UK, 2009).